UvA-DARE (Digital Academic Repository)

Protection of a Gold Catalyst by a Supramolecular Cage Improves Bioorthogonality

James, C.C.; Wu, D.; Bobylev, E.O.; Kros, A.; de Bruin, B.; Reek, J.N.H.

Protection of a Gold Catalyst by a Supramolecular Cage Improves Bioorthogonality

Catriona C. James,[a] Dinghao Wu,[b] Eduard O. Bobylev,[a] Alexander Kros,[b] Bas de Bruin,[a] and Joost N. H. Reek*[a]

Gold catalysts exhibit poor compatibility with cellular components. We show that encapsulation of a gold catalyst within the cavity of a supramolecular cage improves the reactivity of the gold complex under biological conditions. The gold complex catalyzes an intramolecular hydroarylation to produce a fluorescent dye. The encapsulated gold is able to produce this dye in higher yields compared to the free gold under aqueous aerobic conditions and in the presence of biological additives. The substrate was found to be highly cytotoxic, meaning that a very low substrate concentration of 1 μM is required to carry its transformation inside living cells; however, catalysis in cell culture media carried out at micromolar range is found to be inhibited. Although this specific reaction cannot be applied inside living cells, we present a viable strategy to improve the reactivity of gold catalysts in vivo.

Introduction

The selective activation of prodrugs and medicines is highly desirable, as it provides the ability to obtain precise spatial and temporal control over their activity which may minimize off-target reactivity.[1] This is particularly relevant for cancer treatment, where system-wide toxicity goes hand in hand with cancer cell toxicity, often resulting in severe side effects.[2] In order to achieve such selectivity, a bioorthogonal trigger is needed to activate the drug, which should selectivity occur at the desired location. In addition, this trigger should be inert in the off-target cells and should not influence other endogenous processes within the cell. One strategy to accomplish is to design prodrugs which are activated by new-to-nature transformations. Transition metal catalysis is a powerful tool to achieve this as it provides access to a wide scope of reactions which cannot be performed by native enzymes.[3] Gold catalyzed transformations are attractive for this purpose, as they are known to undergo bioorthogonal transformations. For example, gold complexes have been shown to promote C—S

cross coupling reactions in biological systems, whereby aryl groups were conjugated to cysteine residues in bacterial proteins.[4] In addition, they provide routes to synthesize cyclic compounds, a scaffold commonly found in medicines, from alkynes.[5] Alkynes are known to have good bio-orthogonality as they are generally not found naturally in the cell environment, which decreases the chances of non-desired reactivity.[6]

Gold catalyzed cyclizations have already been performed in vivo; however, the activity of the gold catalyst itself is typically very low. The first example of a gold catalyzed intramolecular hydroarylation was shown by Mascareñas and coworkers.[7] Although they showed that only 10 mol% of a small gold catalyst, [Au(PTA)Cl], could successfully convert the substrate to generate a fluorescent coumarin derivative in water with almost quantitative conversion, when the reaction was applied inside HeLa cells the authors estimated a turnover number (TON) of just 1.12. As accurate quantification of catalytic reactions in vitro is challenging, the authors emphasized that this TON should only be taken as an approximation. Yet, it is clear that the cellular environment has a considerable detrimental effect on the activity of the gold complex. The root of this problem is the high concentrations of strongly gold-binding thiol-containing biomolecules, such as glutathione (GSH), present in the cellular environment.[7] A need to protect the gold catalyst from the cellular environment prompted Tanaka et al. to dock an NHC—Au(I) complex inside an albumin scaffold, to generate an artificial metalloenzyme. Indeed, good conversions to generate an anticancer compound were achieved when the gold complex was docked inside the hydrophobic cavity of the protein, whereas the free complex was readily poisoned by thiols and therefore exhibited almost no reactivity. As such, the hydrophilic GSH molecules apparently cannot reach the complex when it is inside the hydrophobic cavity of the protein. In A549 cells it was shown that while high concentrations of gold complex were needed to synthesize the cytotoxic compound and induce cell death,

[a] Dr. C. C. James, Dr. E. O. Bobylev, Prof. B. de Bruin, Prof. J. N. H. Reek
van't Hoff Institute for Molecular Sciences
University of Amsterdam
1098 XH Amsterdam (The Netherlands)
E-mail: j.n.h.reek@uva.nl
Homepage: http://homkat.nl/
[b] D. Wu, Prof. A. Kros
Leiden Institute of Chemistry
Leiden University
Leiden 2333 CC (The Netherlands)

ChemCatChem

Research Article
doi.org/10.1002/cctc.202200942

**Chemistry
Europe**
European Chemical
Societies Publishing

much lower concentrations of metalloenzyme were needed to achieve the same levels of cytotoxicity, indicating that protection of the gold catalyst with the protein scaffold can prevent catalyst poisoning and improve reactivity.[8] This incompatibility of gold complexes with the cellular environment runs both ways. Cellular biomolecules have a detrimental effect on the catalytic activity, but gold complexes can also harm the cells by inducing toxicity themselves. Zou *et al.* therefore developed a system where an inactive and non-toxic gold complex was first applied in cells. This gold complex was activated by a palladium species to become cytotoxic and catalytically active for an intramolecular hydroarylation reaction to synthesize a fluorescent coumarin derivative. This dual activity of the gold complex was demonstrated in both A549 cells and in zebrafish.[9]

Considering the poor compatibility of gold catalysts with the components in living cells, we aimed to design a simple system whereby protection could be provided for both the gold catalyst from the cell environment and the cell from the gold complex. To this end we looked for ways to encapsulate the gold complex in a supramolecular cage, eventually carrying out gold catalysis within the cavity of a cage. The molecular capsule should provide a physical barrier between the gold center and the surrounding environment, leading to improved compatibility. In previous work, gold complexes have been encapsulated with the aim to improve their catalytic properties in terms of activity and selectivity. Reported benefits of confinement on catalysis have been due to: 1) pre-organization of substrate and catalyst;[10] 2) positive effects of increased local concentration of catalysts;[11] 3) cage effects that control the selectivity;[12] and 4) stabilization of the catalyst by the cage.[13] Although there are several examples of gold catalysts being encapsulated in a range of different supramolecular cages,[14] we selected the small tetrahedral $K_{12}[Ga_4L_6]$ cage developed by Raymond and coworkers for the current goal (Figure 1).[15] Once encapsulated inside this cage, catalysts are known to participate in size-selective catalysis, where only substrates small enough to fit through the window are able to react.[12c] With this in

mind, we hypothesized that large biomolecules may be stopped from reaching the gold center, while small substrate molecules may still access the active site. In addition, a gold catalyst, $[Au(PMe_3)]^+$, has been shown to bind inside the cavity of the cage. The encapsulated gold complex exhibited improved activity compared to the free complex,[16] and has also been shown to participate in a tandem reaction with enzymes, indicating its biocompatibility.[17] Here we explore the use of encapsulated gold complexes for catalysis applications under biological conditions in living cells.

Results and Discussion

Approach

The tetrahedral $K_{12}[Ga_4L_6]$ cage (see Figure 1A) was prepared according to a literature procedure, and spectroscopic data were identical to those reported by Raymond *et al.*[16] Preparation of the encapsulated gold complex, $[Au(PMe_3)]^+ \subset cage$, was achieved by mixing 1.2 eq of the cage with 1 eq of the commercially available gold catalyst, $[Au(PMe_3)Cl]$. The catalytically active cationic gold species $[Au(PMe_3)]^+$ resides within the cavity, as the highly negative charged capsule is able to encapsulate cationic guests due to electrostatic interactions. For reactions with free $[Au(PMe_3)Cl]$, no chloride-abstracting reagents were required as it is known that the chloride is able to dissociate from the gold center in water.[7] Catalyst encapsulation in the aqueous phase was established by ^1H NMR spectroscopy and 2D ^1H diffusion ordered NMR spectroscopy (DOSY). Two new overlapping doublets appeared in the ^1H NMR spectrum (Figure S1) at -1.85 and -1.89 ppm which correspond to the phosphine alkyl protons of $[Au(PMe_3)Cl]$, and these peaks are shifted upfield with respect to those of free $[Au(PMe_3)Cl]$, which would appear at 1.64 ppm. Besides this, all the aromatic peaks belonging to the empty cage appear between 7.80 and 6.52 ppm, but in the presence of $[Au(PMe_3)Cl]$ they are all shifted downfield to between 7.84 and 6.57 ppm. In addition, the DOSY spectrum (Figure S3) had only one band with a logD value of -9.62, indicating that only one species is diffusing in solution. Together these data are characteristic of encapsulation of the gold complex within the cavity of the cage. In order to monitor catalytic conversions in the highly complex environment of the cell, typically substrates are used that become fluorescent upon product formation.[18] However, many fluorophores contain large aromatic groups in their structure, which may be too large to fit through the small windows of the cage (see supplementary information). We therefore designed a small alkyne-containing substrate, **1**, which upon a gold catalyzed hydroarylation reaction generates a coumarin dye, **2a**. As a by-product, a non-fluorescent regio-isomer **2b** can also be formed (Figure 1B). Substrate **1** was prepared using standard synthetic steps from commercially available building blocks (see supplementary information). To successfully demonstrate that catalysis can be performed in living cells, we need to: 1) explore the cytotoxicity of the substrate, catalyst, and product, which will set the boundary
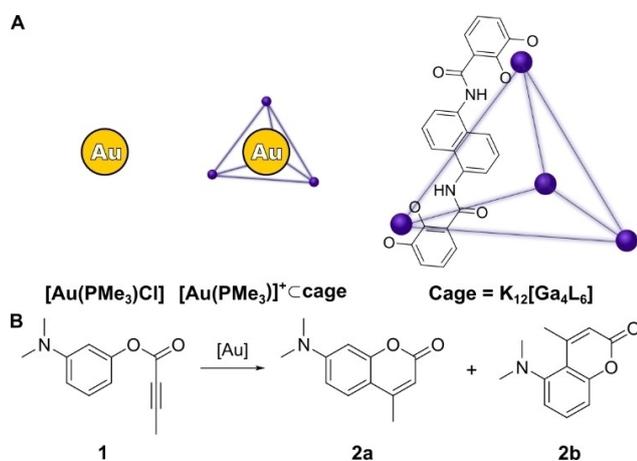

Figure 1. A) Structures of $[Au(PMe_3)Cl]$ and cage. B) Gold catalysed intramolecular hydroarylation of substrate **1** to form fluorescent dye **2a** and the non-fluorescent regio-isomer **2b**.

conditions for catalysis; 2) demonstrate that the caged catalyst enters the living cell in order to perform the catalytic transformation; and 3) explore the compatibility of the catalyst system with commonly abundant components in living cells. In the following sections these will be discussed.

Cytotoxicity and catalyst conditions

Before catalysis can be carried out, appropriate reaction conditions need to be found. The reaction conditions for transition metal catalysis inside cells is often vastly different to that of catalytic reactions for synthetic purposes. While catalysis reactions for synthesis typically are carried out at millimolar to molar concentrations of substrate, much lower concentrations are typically required for catalysis in cells. Ideally, the reaction components for catalysis should induce as little cytotoxicity as possible, in order to ensure that the reaction mainly takes place inside of living cells, rather than extracellularly in the presence of dead cells. Therefore, the biocompatibility of the reaction components with living cells was first investigated in order to determine the appropriate reaction conditions for intracellular catalysis. To this end, the viability of human cervical cancer cells (HeLa cells) was determined in the presence of substrate **1**, product **2a**, the free [Au(PMe$_3$)Cl], the empty cage, and the encapsulated [Au(PMe$_3$)]$^+$⊂cage, using an MTT (3-(4,5-dimethylthiazol-2-yl)-2,5-diphenyltetrazolium bromide) assay (Figure 2). After HeLa cells were incubated with increasing concentrations of the compounds, the percentage of cells which remained alive compared to before incubation with the compounds, was determined. The relative cytotoxicity of the different compounds was determined by comparing the cell viability in the presence of each of the compounds at a given concentration. Substrate **1** was found to induce very high levels of cytotoxicity: at only 10 μM, the cell viability was just 23%. In order to minimize cytotoxicity induced by substrate **1**, it should be
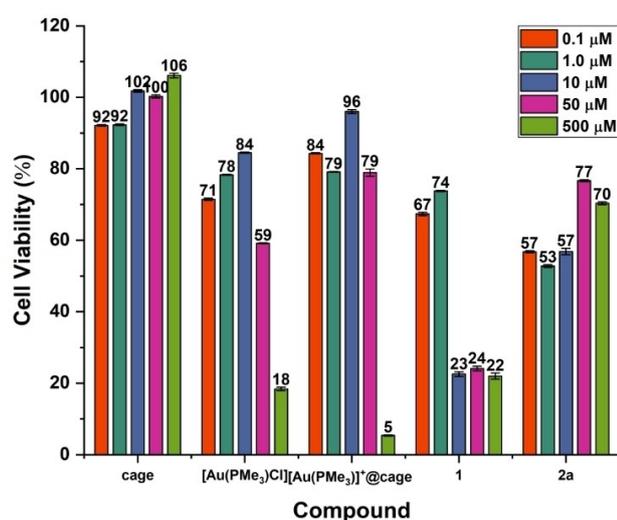
applied in very low concentrations for catalysis, ideally at just 1 μM, as at this concentration a cell viability of 74% was observed. The cell viability of product **2a** at concentrations above 10 μM was higher than that for substrate **1**, and below these concentrations the cell viabilities of substrate **1** and product **2** are similar (67–74% and 57–53% respectively). This means that any product which would be formed during catalysis would not induce any significant cytotoxicity at this concentration. Both of the gold complexes were also found to induce less cytotoxicity than the substrate. Gratifyingly, the encapsulated [Au(PMe$_3$)]$^+$⊂cage complex exhibited reduced cytotoxicity compared to the free [Au(PMe$_3$)Cl]: 79% cell viability was observed for [Au(PMe$_3$)]$^+$⊂cage at 50 μM, while at the same concentration for free [Au(PMe$_3$)Cl] the cell viability was only 59%. The cage itself was essentially non-cytotoxic, even at cage concentrations up to 500 μM. Although the cytotoxicity of the gold complex was reduced by encapsulation within the cage, the lack of cytotoxicity across all concentrations of cage brought into question the cell membrane permeability of the cage. The [Au(PMe$_3$)]$^+$⊂cage complex has a total negative charge of −11, and it is often challenging to transport large hydrophilic or charged cargo across the cell membrane.[19]

Uptake of cages in living cells

Confocal microscopy was used in order to visualize uptake of the cage using fluorescence. As the [Au(PMe$_3$)]$^+$⊂cage complex itself is not fluorescent, the cage was labelled with the fluorescent dye RhodamineB (RhoB), generating a fluorescent RhoB-cage complex. Although RhoB is very large, we hypothesized that electrostatic interactions could bind the dye to the cage, either by partial encapsulation of the alkyl groups within the cavity, or by binding to the exterior of the cage. A solution of 1 eq RhoB and 1.2 eq cage in water was stirred for 30 min at room temperature, and analyzed by ^{1}H NMR spectroscopy, DOSY, UV/Vis spectroscopy, fluorescence spectroscopy, and cryospray ionization high resolution mass spectrometry (CSI-HRMS). In the ^{1}H NMR spectrum of the RhoB and cage mixture (Figure S4), the quartet at 3.49 ppm and the triplet at 1.16 ppm of the free RhoB were shifted upfield and appeared as two broad singlets at 3.06 ppm and 0.94 ppm respectively. In addition, the aromatic signals of the free RhoB between 8.17–6.57 ppm and the aromatic signals of the empty cage between 7.80–6.47 ppm were all shifted to give a set of overlapping peaks between 7.53–6.44 ppm. All of these signals in the RhoB and cage mixture gave one band in the DOSY spectrum with a logD value of −9.63 (Figure S5), indicating that there is one species in solution. In addition, the CSI-HRMS spectrum had signals which correspond to 3-, 4-, and 5- species containing one cage and one RhoB (Figure S7). Finally, the UV/Vis spectrum of RhoB in the presence of cage also indicated binding (Figure S6). The absorption at 554 nm decreased from 1.09 for free RhoB to 0.86 for RhoB in the presence of cage, which is typical for of a binding event. Having established that RhoB indeed binds to the cage, the fluorescence properties of the

Figure 2. MTT assay of reaction components in HeLa cells at different concentrations.

resultant complex was evaluated. Although the RhoB-cage complex indeed displays fluorescence, the intensity of the emission spectrum is lower than that of the free RhoB, indicating that fluorescence of the RhoB is partially quenched upon binding (Figure 3B). Therefore, if fluorescence is detected after incubation with cells with the RhoB-cage complex, comparing the fluorescence intensity with that of the free RhoB gives an indication of whether or not the RhoB is still bound to the cage and therefore shows whether or not the cage has entered the cell. To this end, HeLa cells were incubated with a 1 μM solution of either RhoB or RhoB-cage for 30 min, followed by washing twice with PBS buffer. While fluorescence was observed in the cytoplasm of the cells incubated with free RhoB, only background fluorescence was seen for the RhoB-cage (Figure 3C). Therefore, the cage together with its cargo is not cell permeable, and the reason for the cage being non-toxic is due to the fact that it does not in fact enter the cell. This means that in order to carry out the reaction inside cells, the $[Au(PMe_3)]^+ \subset cage$ complex would need to be first brought into the cell using a cell-penetrating vehicle, such as a cell-penetrating peptide or lipid nanoparticle (LNP).

Effect of catalyst encapsulation on biocompatibility

In order to gain insights into catalytic conversion of substrate **1** under biologically relevant conditions, we first carried out the catalysis at high substrate concentrations, under the typical catalysis conditions used in the literature for $[Au(PMe_3)]^+ \subset cage$.[16,17] Therefore 0.2 M of substrate **1** was stirred at 37 °C for 16 h in the presence of 2.5 mol% catalyst. Almost identical yields of the fluorescent product **2a** were obtained for both free $[Au(PMe_3)Cl]$ and encapsulated $[Au(PMe_3)]^+ \subset cage$ in water, with 69% and 70% yields respectively (Figure 4A). Due to solubility reasons, the reaction mixtures could not be analyzed by ^1H NMR spectroscopy, and the yield of **2a** was instead determined by fluorescence intensity: the concentration of product **2a** was calculated from a fluorescence calibration curve, and the final yield determined from the ratio between the observed concentration and theoretical maximum concentration of product **2a**. When the catalysis was carried out in CH_3CN using $[Au(PPh_3)Cl]$ as catalyst, full conversion was achieved, resulting in a 7:3 ratio of fluorescent product **2a** and the non-fluorescent regio-isomer **2b**. Therefore, it is likely that **2b** is also being formed during the catalysis water, and that the overall conversion is higher than the yield of **2a**. Having established the successful formation of **2a** by $[Au(PMe_3)]^+ \subset cage$, we next looked to investigate the effect of the in the
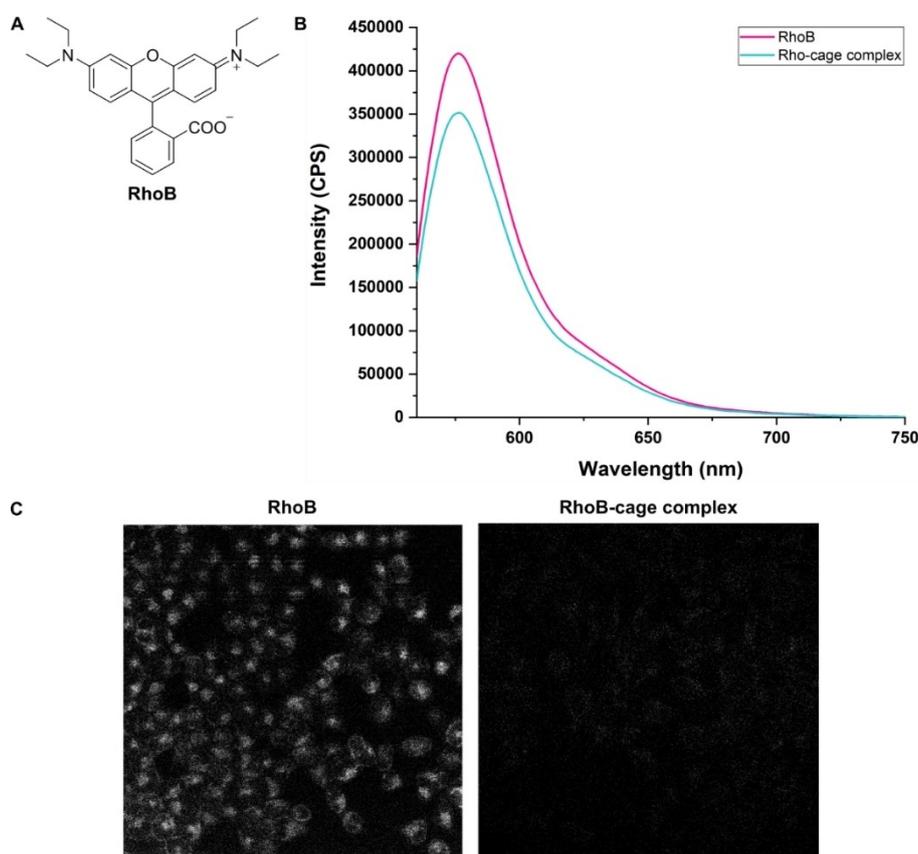

Figure 3. A) Structure of RhoB. B) Emission spectra of a 1 μM solution of RhoB and a 1 μM solution of RhoB-cage complex in water. C) Confocal microscopy images of HeLa cells incubated with a 500 nM solution of RhoB or RhoB-cage complex.
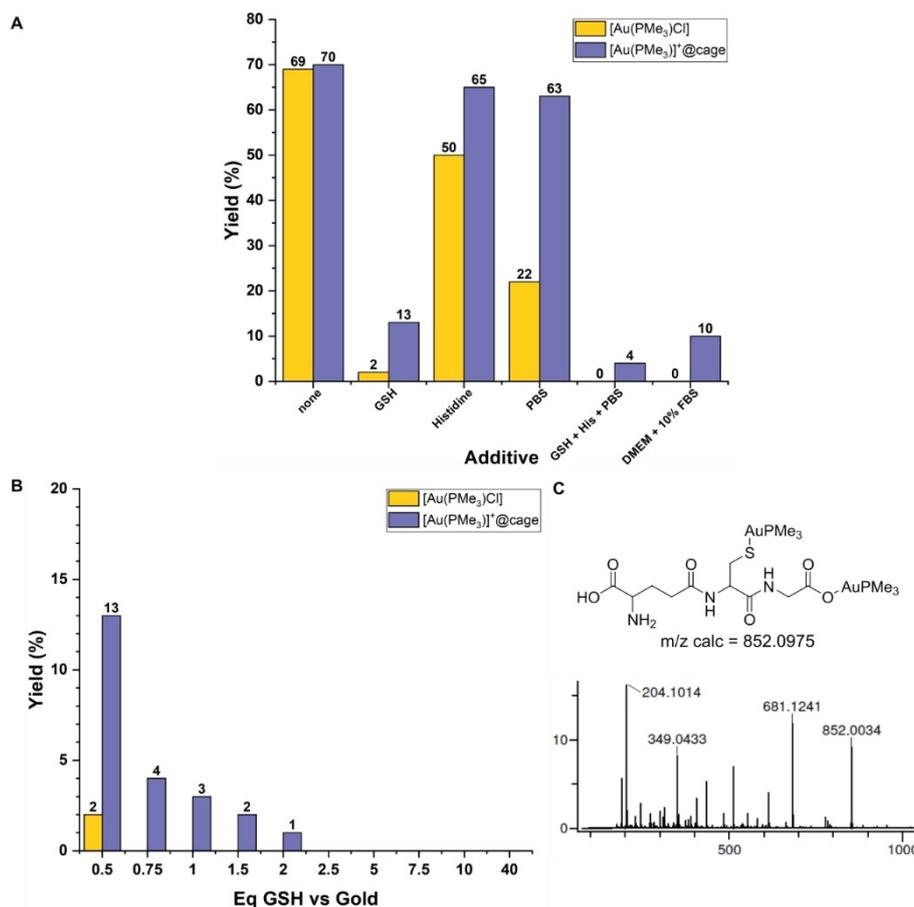
ChemCatChem

Research Article
doi.org/10.1002/cctc.202200942

Chemistry
Europe
European Chemical
Societies Publishing

Figure 4. A) Yields of product **2** after Catalysis of substrate **1** with free [Au(PMe₃)Cl] and encapsulated [Au(PMe₃)]⁺⊂cage in the presence of biological additives. B) Yields of product **2** after catalysis of substrate **1** with free and encapsulated catalyst in the presence of increasing equivalents of GSH. C) ESI-HRMS spectrum (positive mode) of the catalysis reaction mixture in the presence of 0.5 equivalents of GSH with respect to gold.

presence of biological additives; namely GSH, and L-histidine (His), an amino acid which contains a metal-binding imidazole moiety, and PBS buffer. 2.5 mol% of either free [Au(PMe₃)Cl] or encapsulated [Au(PMe₃)]⁺⊂cage was first mixed with 1.25 mol% His or GSH in water before addition of substrate **1**, and the resulting mixture was stirred at 37 °C for 16 h. In all cases, the encapsulated [Au(PMe₃)]⁺⊂cage complex outperformed free [Au(PMe₃)Cl]. Histidine had the least effect upon the catalytic activity of the gold, with a 50% yield of **2a** for free [Au(PMe₃)Cl] and 65% yield for encapsulated [Au(PMe₃)]⁺ ⊂cage. The presence of PBS buffer had an inhibiting effect upon catalysis. When the reaction was carried out in a 8:2 mixture of PBS/water, the yield dropped to just 22% for free [Au(PMe₃)Cl] while it remained high for encapsulated [Au-(PMe₃)]⁺⊂cage, at 63%. While the high concentration of chlorides in the PBS buffer (140 mM) disfavors dissociation of the chloride from the free [Au(PMe₃)Cl] complex and therefore reduces the amount of active species in solution, it appears that this is not the case in the presence of the cage: once encapsulated inside the cage, recombination of the gold center with the chloride is prevented. As expected, GSH behaved as a strong poison for the catalysis. Even in the presence of only

0.5 eq of GSH compared to the gold, free [Au(PMe₃)Cl] only generated **2a** in a 2% yield. However, upon encapsulation a 6-fold increase in yield was observed, with a 13% yield for [Au(PMe₃)]⁺⊂cage. When the reaction mixture was analyzed by high resolution electrospray ionization mass spectrometry (Figure 4C), a peak at 852.0034 was observed, which corresponds to a species containing one GSH molecule and two [Au(PMe₃)]⁺ cations. No species corresponding to one GSH molecule and one [Au(PMe₃)]⁺ cation was observed. It appears that one GSH molecule poisons the catalysis by binding two gold centers. As GSH is found in concentrations of 2–5 mM in cells,[20] we looked to see the extent to which the cage could protect against this thiol poisoning. Catalysis was carried out in the presence of increasing equivalents of GSH with respect to the gold, and, unsurprisingly, no yield at all of **2a** was observed above 0.5 eq for free [Au(PMe₃)Cl] (Figure 4B). However, for the [Au(PMe₃)]⁺ ⊂cage complex **2a** was still observed with up to 2 eq of GSH, albeit in very low yields (<5%). Catalysis was also carried out in the presence of all three biological additives combined. When both GSH and His are combined together in PBS buffer no yield at all is observed for free [Au(PMe₃)Cl], however **2a** was still produced in a 4% yield for the encapsulated [Au(PMe₃)]⁺

ChemCatChem

Research Article
doi.org/10.1002/cctc.202200942

Chemistry
Europe
European Chemical
Societies Publishing

⊂cage. Finally, catalysis was also carried out in the presence of cell culture medium (DMEM + 10% FBS), as such media contains a complex mixture of proteins and biomolecules, which is similar to what is found inside of cells. Using free [Au(PMe₃)Cl] again resulted no yield; however, encapsulated [Au(PMe₃)]⁺ ⊂cage was able to generate **2a** in a 10% yield. It is likely that the lower yields observed when DMEM + 10% FBS was used as solvent compared to water is again due to poisoning from thiols found in the amino acids and proteins in the cell culture medium. Although the catalytic activity of encapsulated [Au-(PMe₃)]⁺⊂cage is quite drastically reduced in the presence of these biological additives, **2a** is still generated in consistently higher yields compared to free [Au(Me₃P)Cl]. Therefore, while poisoning still takes place, the cage indeed is able to provide some protection against these biological additives. While it is clear that GSH is one source of catalysis inhibition under biological conditions, it should be noted that while these data give an indication of what may happen *in vivo*, they may not necessarily translate to the cell environment; the cell is a highly complex, heterogeneous environment,[21] and such simple test reactions under physiological conditions may not paint an accurate picture of how the system will behave inside a cell. The reactivity of gold catalysts towards a variety of transformations, including hydroarylations, has been shown to be highly dependent on the counterion of the gold complex;[22] for example, DFT studies into a propargylic amide cyclization using an LAuNTf₂ complex as catalyst show that (NTf₂)⁻ counterions interact with the amide group to promote (de-)protonation during the catalytic cycle.[23] Therefore it is highly possible that the reactivity of the encapsulated and free gold complexes may be different if the chloride counterion is substituted by other anions found in the cell.

With the promising results of gold catalyst protection from typical biological metal poisons by encapsulation in the gallium-cage and established cytotoxicity of substrate **1**, next the biocompatibility of the reaction itself was investigated under the required concentrations of all components. The reaction was carried out under physiological conditions, rather than in cells, in order to gain insight into how the reaction behaves in the presence of biological components, as both the set-up and analysis is more facile under physiological conditions compared to in cells. Catalysis was therefore carried out under dilute conditions in various cell culture media in order to determine if the reaction would be feasible *in vivo* (Table S2, SI). Solutions of the catalysts were first prepared in water or DMSO before addition of the substrate. A solution of 50 mol% of either encapsulated [Au(PMe₃)]⁺⊂cage in water or free [Au(PMe₃)Cl] in DMSO was therefore added to cell culture media (either DMEM + 10% FBS, FBS, or FBS/PBS mixtures), followed by the addition of 1 eq of substrate **1** to give a final concentration of 10 μM of substrate. This concentration of substrate was selected so that even at low yields, product **2a** would still be able to be detected. The reaction mixtures were stirred at 37 °C for 16 h, after which they were directly analyzed by fluorescence spectroscopy. Unfortunately, in all cases, for both encapsulated [Au(PMe₃)]⁺⊂cage and free [Au(PMe₃)Cl], no fluorescence was detected, meaning that no product was formed. Therefore,

catalysis with either free or encapsulated gold is not possible under the conditions which would be required for in cells. While we demonstrated clearly a protective effect of the nanocage for encapsulated gold catalyst under semi-biological conditions in the presence of biological metal poisons, further substrate design and optimization is required for the application of such systems in living matter.

Conclusion

An encapsulated gold catalyst was able to catalyze an intramolecular hydroarylation reaction to produce a fluorescent coumarin dye. Under catalytic conditions in water the encapsulated [Au(PMe₃)]⁺⊂cage complex was able to generate the product with about the same yields as the free catalyst. Importantly, under identical conditions in the presence of biological additives such GSH, Histidine, PBS buffer, and cell culture medium, the encapsulated catalyst [Au(PMe₃)]⁺⊂cage provided much higher yields than the free [Au(PMe₃)Cl], indicating the cage was providing protection for the gold catalyst. The [Au(PMe₃)]⁺⊂cage complex afforded product **2a** in the presence of GSH, His, PBS buffer, and cell culture medium, whereas free [Au(PMe₃)Cl] was completely inactive under the same conditions. Although the proof of principle that catalyst protection can be achieved by encapsulation in synthetic molecular cages, several issues need to be solved before these systems can be applied in cells. At very low substrate concentrations (10 μM) required for reactions to be carried out in cells, neither the free [Au(PMe₃)Cl] nor encapsulated [Au(PMe₃)]⁺⊂cage was able to generate product **2a** in cell culture media, so activity or stability under these conditions need to be improved. The cage itself was found to be not cell permeable and vehicles known to transport non-permeable cargo into cells may be required.[24] For example, encapsulation of the [Au(PMe₃)]⁺⊂cage complex inside lipid nanoparticles (LNPs) may provide a viable route to deliver the protected catalyst into the cell.[25] Another potential route to cell permeability may be bioconjugation of the cage to a cell penetrating peptide, a strategy which has previously been applied to Pd₂L₄ metallocages.[26] Also, the substrate should be redesigned as such so that it is less toxic and can be used at higher substrate concentrations. In addition, an even smaller substrate may further improve the protection provided by the cage, and further enhance the activity of the encapsulated gold under biological conditions.

Experimental Section

Cell experiments

HeLa cells were incubated for 30 min with RhoB or RhoB-cage complex in DMEM + 10% FBS to give a final concentration of 500 nM. The cells were then washed 3 times with PBS and then imaged by confocal microscopy.

ChemCatChem

Research Article
doi.org/10.1002/cctc.202200942

Chemistry Europe
European Chemical
Societies Publishing

General procedure for catalysis

An aqueous solution of cage (3 mol%) was added to solid [Au(PMe$_3$)Cl] (2.5 mol%) and stirred at room temperature for 30 min. Either the desired solvent or an aqueous solution of the desired additive was then added, followed by neat substrate (1 eq). This solution was stirred at 37 °C for 16 h. The yield of **2a** was determined by diluting the reaction mixture with DMSO and measuring the fluorescence intensity.

Full experimental procedures are described in the supplementary information.

Acknowledgements

Conflict of Interest

The authors declare no conflict of interest.

Data Availability Statement

The data that support the findings of this study are available from the corresponding author upon reasonable request.

[1] J. Rautio, N. A. Meanwell, L. Di, M. J. Hageman, *Nat. Rev. Drug Discovery* **2018**, *17*, 559–587.

[2] C. Souza, D. S. Pellosi, A. C. Tedesco, *Expert Rev. Anticancer Ther.* **2019**, *19*, 483–502.

[3] a) M. O. N. van de L'Isle, M. C. Ortega-Liebana, A. Unciti-Broceta, *Curr. Opin. Chem. Biol.* **2021**, *61*, 32–42; b) R. C. Brewster, E. Klemencic, A. G. Jarvis, *J. Inorg. Biochem.* **2021**, *215*, 111317; c) M. J. S. A. Silva, P. M. P. Gois, G. Gasser, *ChemBioChem* **2021**, *22*, 1740–1742; d) Z. Chen, H. Li, Y. Bian, Z. Wang, G. Chen, X. Zhang, Y. Miao, D. Wen, J. Wang, G. Wan, *Nat. Nanotechnol.* **2021**, *16*, 933–941; e) B. Lozhkin, T. R. Ward, *Bioorg. Med. Chem.* **2021**, *45*, 116310; f) T. Völker, E. Meggers, *Curr. Opin. Chem. Biol.* **2015**, *25*, 48–54; g) M. Martínez-Calvo, J. L. Mascareñas, *Coord. Chem. Rev.* **2018**, *359*, 57–79.

[4] a) M. N. Wenzel, R. Bonsignore, S. R. Thomas, D. Bourissou, G. Barone, A. Casini, *Chem. Eur. J.* **2019**, *25*, 7628–7634; b) C. Schmidt, M. Zollo, R. Bonsignore, A. Casini, S. M. Hacker, *Chem. Commun.* **2022**, *58*, 5526.

[5] a) Z. Li, C. Brouwer, C. He, *Chem. Rev.* **2008**, *108*, 3239–3265; b) A. S. K. Hashmi, M. Rudolph, *Chem. Soc. Rev.* **2008**, *37*, 1766–1775; c) Y. Zhang, T. Luo, Z. Yang, *Nat. Prod. Rep.* **2014**, *31*, 489–503; d) M. Rudolph, A. S. K. Hashmi, *Chem. Soc. Rev.* **2012**, *41*, 2448–2462.

[6] M. E. Ourailidou, M. R. H. Zwinderman, F. J. Dekker, *MedChemComm* **2016**, *7*, 399–408.

[7] C. Vidal, M. Tomás-Gamasa, P. Destito, F. López, J. L. Mascareñas, *Nat. Commun.* **2018**, *9*, 1913.

[8] T.-C. Chang, K. Vong, T. Yamamoto, K. Tanaka, *Angew. Chem.* **2021**, *133*, 12554–12562.

[9] Y. Long, B. Cao, X. Xiong, A. S. C. Chan, R. W.-Y. Sun, T. Zou, *Angew. Chem. Int. Ed.* **2021**, *60*, 4133–4141; *Angew. Chem.* **2021**, *133*, 4179–4187.

[10] a) Q.-Q. Wang, S. Gonell, S. H. A. M. Leenders, M. Dürr, I. Ivanović-Burmazović, J. N. H. Reek, *Nat. Chem.* **2016**, *8*, 225–230; b) F. Yu, D. Poole III, S. Mathew, N. Yan, J. Hessels, N. Orth, I. Ivanović-Burmazović, J. N. H. Reek, *Angew. Chem. Int. Ed.* **2018**, *57*, 11247–11251; *Angew. Chem.* **2018**, *130*, 11417–11421.

[11] a) R. Gramage-Doria, J. Hessels, S. H. A. M. Leenders, O. Tröppner, M. Dürr, I. Ivanović-Burmazović, J. N. H. Reek, *Angew. Chem. Int. Ed.* **2014**, *53*, 13380–13384; *Angew. Chem.* **2014**, *126*, 13598–13602; b) S. H. A. M. Leenders, M. Dürr, I. Ivanović-Burmazović, J. N. H. Reek, *Adv. Synth. Catal.* **2016**, *358*, 1509–1518; c) S. Gonell, X. Caumes, N. Orth, I. Ivanović-Burmazović, J. N. H. Reek, *Chem. Sci.* **2019**, *10*, 1316–1321.

[12] a) D. H. Leung, D. Fiedler, R. G. Bergman, K. N. Raymond, *Angew. Chem. Int. Ed.* **2004**, *43*, 963–966; *Angew. Chem.* **2004**, *116*, 981–984; b) D. H. Leung, R. G. Bergman, K. N. Raymond, *J. Am. Chem. Soc.* **2006**, *128*, 9781–9797; c) D. H. Leung, R. G. Bergman, K. N. Raymond, *J. Am. Chem. Soc.* **2007**, *129*, 2746–2747; d) S. S. Nurttila, W. Brenner, J. Mosquera, K. M. van Vliet, J. R. Nitschke, J. N. H. Reek, *Chem. Eur. J.* **2019**, *25*, 609–620.

[13] a) C. J. Brown, G. M. Miller, M. W. Johnson, R. G. Bergman, K. N. Raymond, *J. Am. Chem. Soc.* **2011**, *133*, 11964–11966; b) D. M. Kaphan, M. D. Levin, R. G. Bergman, K. N. Raymond, F. D. Toste, *Science* **2015**, *350*, 1235; c) M. Otte, P. F. Kuijpers, O. Troeppner, I. Ivanović-Burmazović, J. N. H. Reek, B. de Bruin, *Chem. Eur. J.* **2013**, *19*, 10170–10178; d) C. Tan, J. Jiao, Z. Li, Y. Liu, X. Han, Y. Cui, *Angew. Chem. Int. Ed.* **2018**, *57*, 2085–2090; *Angew. Chem.* **2018**, *130*, 2107–2112; e) J. Jiao, C. Tan, Z. Li, Y. Liu, X. Han, Y. Cui, *J. Am. Chem. Soc.* **2018**, *140*, 2251–2259.

[14] A. C. H. Jans, X. Caumes, J. N. H. Reek, *ChemCatChem* **2019**, *11*, 287–297.

[15] D. L. Caulder, R. E. Powers, T. N. Parac, K. N. Raymond, *Angew. Chem. Int. Ed.* **1998**, *37*, 1840–1843; *Angew. Chem.* **1998**, *110*, 1940–1943.

[16] Z. J. Wang, C. J. Brown, R. G. Bergman, K. N. Raymond, F. D. Toste, *J. Am. Chem. Soc.* **2011**, *133*, 7358–7360.

[17] Z. J. Wang, K. N. Clary, R. G. Bergman, K. N. Raymond, F. D. Toste, *Nat. Chem.* **2013**, *5*, 100–103.

[18] a) P. Destito, C. Vidal, F. López, J. L. Mascareñas, *Chem. Eur. J.* **2021**, *27*, 4789–4816; b) S.-Y. Jang, D. P. Murale, A. D. Kim, J.-S. Lee, *ChemBioChem* **2019**, *20*, 1498–1507; c) Y. G. Bai, J. F. Chen, S. C. Zimmerman, *Chem. Soc. Rev.* **2018**, *47*, 1811–1821; d) J. J. Soldevila-Barreda, N. Metzler-Nolte, *Chem. Rev.* **2019**, *119*, 829–869.

[19] V. S. Dave, D. Gupta, M. Yu, P. Nguyen, S. Varghese Gupta, *Drug Dev. Ind. Pharm.* **2017**, *43*, 177–189.

[20] H. J. Forman, H. Zhang, A. Rinna, *Mol. Aspects Med.* **2009**, *30*, 1–12.

[21] D. P. Nguyen, H. T. H. Nguyen, L. H. Do, *ACS Catal.* **2021**, *11*, 5148–5165.

[22] J. Schießl, J. Schulmeister, A. Doppiu, E. Wörner, M. Rudolph, R. Karch, A. S. K. Hashmi, *Adv. Synth. Catal.* **2018**, *360*, 2493–2502.

[23] Y. Ma, H. S. Ali, A. A. Hussein, *Catal. Sci. Technol.* **2022**, *12*, 674.

[24] L. van der Koog, T. B. Gandek, A. Nagelkerke, *Adv. Healthcare Mater.* **2022**, *11*, 2100639.

[25] a) F. Campbell, F. L. Bos, S. Sieber, G. Arias-Alpizar, B. E. Koch, J. Huwyler, A. Kros, J. Bussmann, *ACS Nano* **2018**, *12*, 2138–2150; b) Y. Hayashi, M. Takamiya, P. B. Jensen, I. Ojea-Jiménez, H. Claude, C. Antony, K. Kjaer-Sorensen, C. Grabher, T. Boesen, D. Gilliland, *ACS Nano* **2020**, *14*, 1665–1681; c) G. Arias-Alpizar, L. Kong, R. C. Vlieg, A. Rabe, P. Papadopoulou, M. S. Meijer, S. Bonnet, S. Vogel, J. van Noort, A. Kros, *Nat. Commun.* **2020**, *11*, 3638; d) C. M. Hong, M. Morimoto, E. A. Kapustin, N. Alzakhem, R. G. Bergman, K. N. Raymond, F. D. Toste, *J. Am. Chem. Soc.* **2018**, *140*, 6591–6595.

[26] J. Han, A. Schmidt, T. Zhang, H. Permentier, G. M. M. Groothuis, R. Bischoff, F. E. Kühn, P. Horvatovich, A. Casini, *Chem. Commun.* **2017**, *53*, 1405.